Vortex Breakdown - Investigations by using the Ultrasonic-Laser-Method and Laser-Sheet Technique

by R.H. Engler

Deutsche Forschungs- und Versuchsanstalt für Luft- und Raumfahrt e.V. (DFVLR)

Göttingen, West Germany

Summary

An ultrasonic-laser measuring system has been developed which is usefull for fast and nondisturbing exploration of the flow field around models in wind tunnels, especially velocity, vorticity, circulation distribution and the stability of vortices.
This technique is based on the measurement of flow-induced travel time differences of short ultrasonic pulses, propagating along a measuring sound beam between two or more laser beams. Particularly the "vortex breakdown" of leading edge vortices has been investigated. Furthermore the method's capability is shown for evaluating instabilities on the rolled up shear layer. A video film, photographs and measurements confirm this facts.

Introduction

The present work employs an opto-acoustic method [1,2] for investigations of the vortex breakdown phenomenon. This phenomenon is very sensitive to the insertion of probes into the flow field and therefore non-contact methods have been preferred such as LDA. Even this previously employed conventional optical method is subject to substantial limitation (lack of scatter particles) when used to investigate the vortices of present interest.

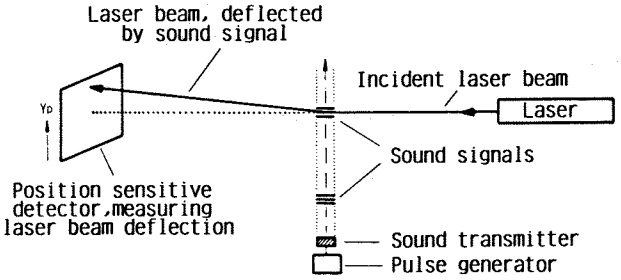

Fig. 1: Schematic diagramm of the test setup for opto-acoustical measurements

With the aid of the opto-acoustical method we possess a tool to investigate these very special cases with a high degree of accuracy. The principle of this method is depicted in figure 1.

Principle of the Opto-Acoustic Method

Years ago, a report [3] has been presented concerning the development of an acoustical method for fast detection and measurement of vortices in wind tunnels. By the new method an optical arrangement as pictured in figure 1 is appropriate to record the density fluctuations of an ultrasonic pulse. A laser beam is sent through the sound beam, perpendicular to the direction of propagating of the sound waves , and reacts to the density gradient caused by the passing sound wave with deflections in y -direction which, in the position sensitive detector, are translated into proportional electrical current.

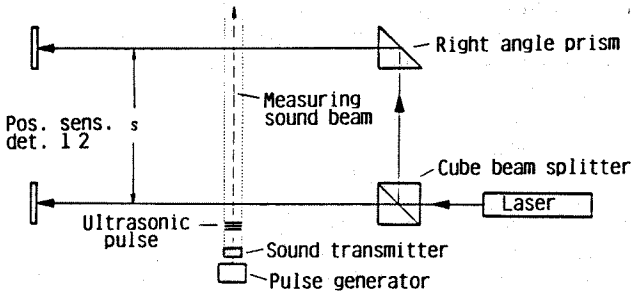

Fig. 2: Arrangement of two laser beams according to figure 1 to set an integration path s within the flow under test

With this method the arrival of ultrasonic pulses can be registered at practically any given point, even within the flow under investigation, without affecting the flow or the ultrasonic signal being affected.
If therefore, according to figure 2, the sonic beam is allowed to cross consecutively two parallel laser beams at a distance s apart, one obtains two received signals

which are staggered by a travel time needed for the ultrasonic pulse to run through the path s. In order to be far outside the range of typical frequencies of sound or turbulence present in any wind tunnel (up to 50 kHz) a frequency of 150 kHz ultrasound was chosen with two periods of oszillation. By correlating these two - digitally stored - signals , a typical example of which is shown in figure 3, the travel time and thus the line integral over the flow velocity along the path s can be determined from the passage of a single ultrasonic pulse. One can make the integration path set optically within the flow very short and thus practically take local velocity measurements punctiformly.

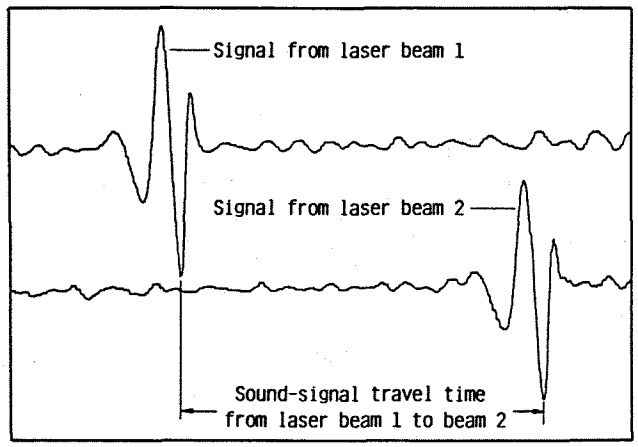

Fig. 3: Received sound signals from both laser beams shown in figure 2. The travel time is obtained from cross correlation of both signals

Experiments of this kind with an integration path of 10 mm , where the achieved accuracy of the travel time difference measurement of 0.4 *10 -8 s allows even the low flow velocity of 5 cm/s to be detected. In addition, tests with an integration path of only 5 mm - and hence comparable with the magnitude of conventional pressure probes- confirmed the resulution of 10 cm/s to be expected in this case.

Experimental Arrangement and Wind Tunnel Tests

As is wellknown, the vortices developing from the leading edge of an inclined slender delta wing are, in general, subject to the so-called vortex breakdown.

This phenomenon by which the regular vortex structure is suddenly lost at a certain downstream position, is extremely sensitive to disturbances emanating from even smallest probes inserted in the flow. Thus, reliable results of measurements cannot be obtained by applying usual probe techniques. Furthermore, investigating vortex flows, one mostly cannot take advantage of the laser-Doppler-anemometry which, as desired, requires no probes in the flow by light scattering particles: such particles are ejected out of the central region of the vortex by centrifugal forces.

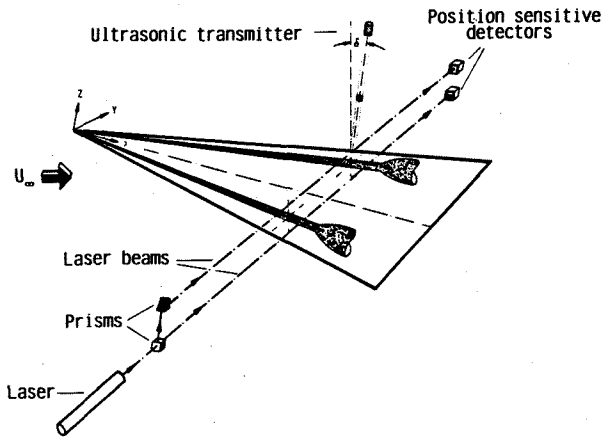

Fig. 4: Test setup for the investigation of vortices adjacent to an inclined slender delta wing, using the opto-acoustical method according to figure 2 to study their internal structure and breakdown

The nondisturbing opto-acoustic method of measurements overcome both disadvantages. The test setup is schematically pictured in figure 4. It shows essentially at its top, far outside the vortices, the ultrasonic transmitter and the optical arrangement needed to employ the two-laser beam method. This apparatus enabled investigations some exemplary results of which may be presented in the following.

The vortex model was a delta wing with a chord length of $\ell = 70$ cm and 56 cm span, corresponding to an aspect ratio of $\Lambda = 1.6$. At a flow velocity of $U_\infty = 20$ m/s the point of vortex breakdown was located at $x/\ell = 0.73$. To investigate the streamwise vortex core development, measurements were performed in seven different x,y-planes upstream of the point of vortex breakdown. Within each plane the sound beam was shifted in steps of $\Delta y = 2$ mm. These relatively small steps thus permit a small scale resolution of the vortex structure.

Theoretical Background

According to figure 5 a sound beam will be shifted successively in the y-direction across the vortex. During this shift, the travel time of a sound signal propagating along the sound beam between the two laser beams 1 and 2 gives the travel time of the signal over a distance s [1] as follows:

$$t_1 = \frac{1}{c} \int_{-\frac{s}{2}}^{+\frac{s}{2}} \frac{dz}{1 - \frac{1.4 r_0 v_{max} y^*}{c (y^{*2} + z^2)} \left\{ 1 - \exp\left[\frac{-1.26 (y^{*2} + z^2)}{r_0^2} \right] \right\}} \qquad (1)$$

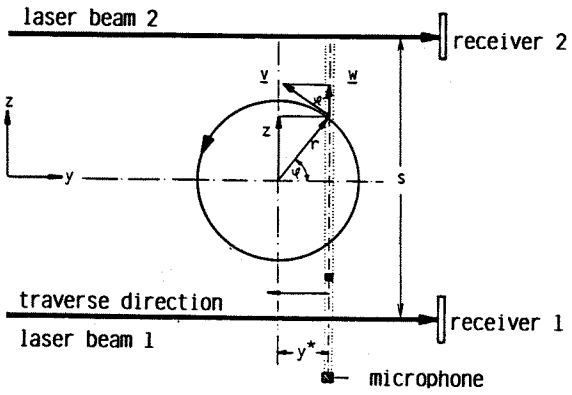

Fig. 5: Principle of the opto-acoustical measurement of flow fields. Sketch for calculation of the travel time of an ultrasonic pulse traversing along the measuring sound beam

The travel time of this signal is changed (reduced due to the tailwind, enlarged due to the headwind) on its way from laser beam 1 to laser beam 2 by flow velocity components present in the signal's direction of propagation. In this vortex model - the Hamel-Oseen vortex - the velocity, closely similar to the realistic case, follows a smooth transition from linear increase at the centre of the vortex to a decrease inversely proportional to the radius at greater distance from the core, in accordance with a potential vortex.
The symbols used here are c= sound velocity, ro= vortex core radius, vmax= maximum circumferential velocity of the vortex and s= distance from laser beam 1 to laser beam 2. Variations of y* produces the profile pictured in figure 6.

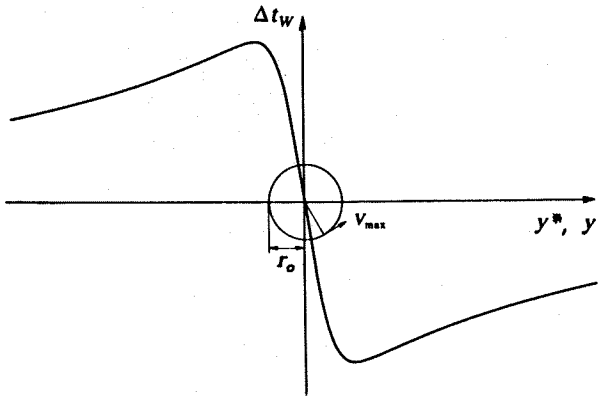

Fig. 6: Calculated travel time differences of ultrasonic pulses produced by a Hamel-Oseen vortex according to figure 5

The corresponding circulation for the Hamel-Oseen vortex expressed by the relation is

$$v_{max} = \frac{0.716\ \Gamma_0}{2\pi r_0} \qquad (2)$$

Within the spiral of the shear layer rolled up in a vortex except the core (for details see figure 9) there is potential flow, the circumferential velocity here is given by

$$v(r,t) = \frac{\Gamma}{2\pi r} \qquad (3)$$

and the travel time for each region between the spiral in this vortex model of the sound signal is

$$t'_i = \frac{2}{c} \int_{+s_i}^{+s_i} \frac{dz}{1 - \frac{(\Gamma_0 + \Delta\Gamma_i) \cdot y^*}{2\pi c(y^{*2} + z_i^2)}} \qquad (4)$$

The flow induced portion then is

$$\Delta t_W = t_0 - (t_1 + t'_i) = f(y^*, r_n, \Gamma_0, \Delta\Gamma_i) \qquad (5)$$

Figure 7 shows a characteristic sample of a plot of travel time differences (Δt_W =DTW) measured by shifting the measuring sound beam through the vortex in front of the point of vortex breakdown. The travel time difference Δt_W was calculated by signal correlation.

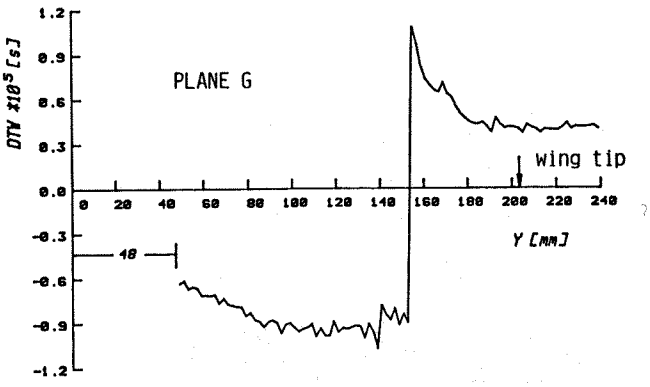

Fig. 7: Measured data for plane G.
Test parameters: U_∞= 20 m/s, α= 28°40', s= 50 mm, x/ℓ= 0.73

Figure 8 demonstrates how accurately measured data can be produced. The measurement was repeated after 30 min wind off. It is truly amazing how accurately significant extrema recur. It can be realized that there are characteristic kinks in the curve which globally decreases.The different measured planes are pictured in figure 10.

Especially the largest kink marks the influence of the leading edge in the roll up process of the shear layer. This kink is well known and has been found by various other measuring techniques.

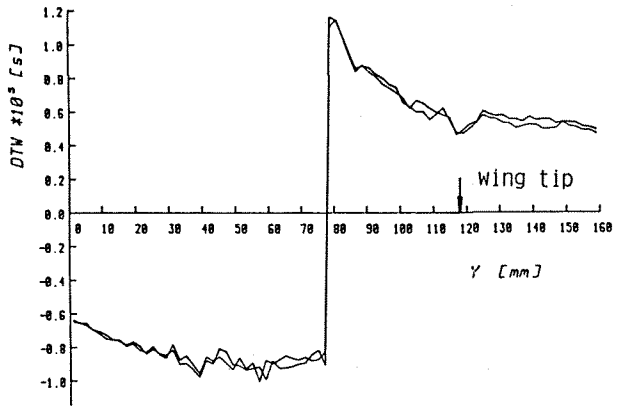

Fig. 8: Repeatebility check in plane C ($x/\ell = 0.614$) measurements where repeated after 30 min wind off and starting again

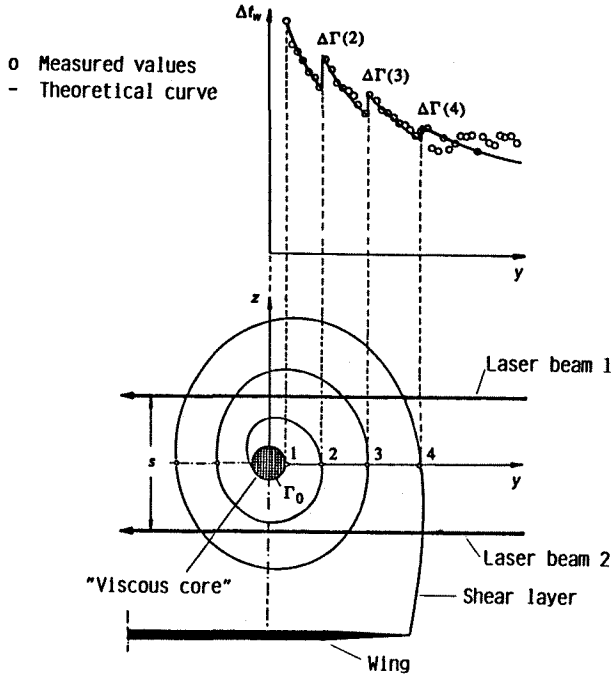

Fig. 9: Upper part: Example of a travel time profile, measured by the method shown in figure 2 , and best fit line calculated on the assumption of potential flow between the measured circulation Γ and the also measured jumps of circulation ΔΓ(2), ΔΓ(3), ΔΓ(4) due to the turns of the rolled up shear layer. Lower part: Sketch of the internal structure of the vortex as derived from the top curve

Vortex Model and Result

The vortex model is based on a combination of a Hamel-Oseen vortex with a viscous core and semi-circle pieces of potential vortices in outer region, with a circulation of $\Delta\Gamma i$ each.

Figure 9 demonstrates the successful detection of the inner structure of a vortex at a position upstream of the breakdown point. The jumps, clearly discernible along the measured circulation curve, correspond to the point where the shear layer which is rolled up forming the vortex crosses the horizontal plane through the vortex

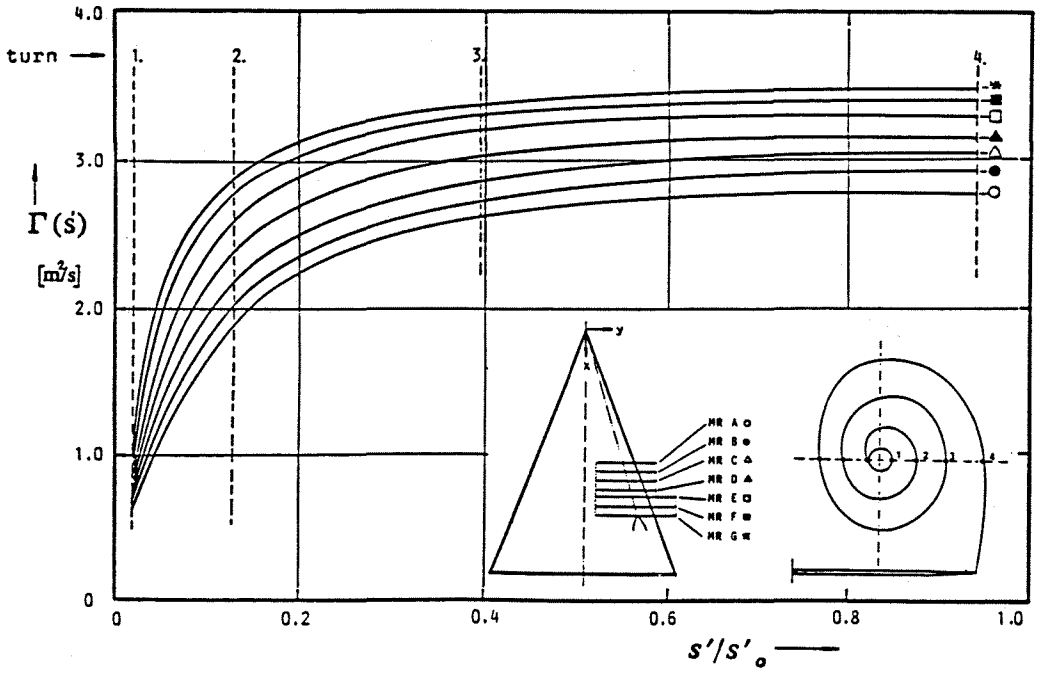

Fig.10: Variation of circulation Γ along the spiral shear layer from vortex core to leading edge (total length of the spiral = s'o)

core. Under the assumption that the flow between the successive turns of the shear layer can be considered as a potential flow, computer-aided curve fitting, as is seen, led to good results of vortex parameters (core radius, circumferential velocity, position and circulation).

From the theoretical curves thus obtained the increase of circulation along the spiral proceeding from the edge of the viscous core to the leading edge of the wing for seven different maesurement rows is shown in figure 10. A further remarkable result obtained from the evaluation of the measured data is a new confirmation of the Ludwieg [4] and Hall [5] stability theory concerning the vortex breakdown.

This theory states a decreasing from parameter K to reach the value 1.16 when, advancing downstream, one arrives at the point where this phenomenon suddenly takes place.

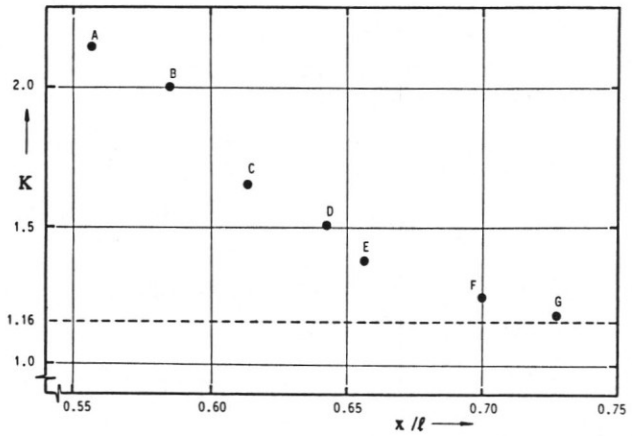

Fig. 11: Ludwieg's parameter of stability K as a function of the distance x/ℓ

In figure 11 values of K are plotted at several downstream positions. Before the measurements where started, a laser sheet technique was employed to find the location of vortex breakdown. Plane G was established just upstream of this position, and final result has shown that the shape parameter in this plane is K = 1.16.

Presentation and Discussion of Flow Visualization by Laser-Light Sheet Technique

The photographs presented in figure 12-15 where reproduced from video tape using a video camera with short exposure time. The illumination system was composed of a 2W Argon-Ion-laser and a cylindrical lens to generate a plane sheet of light. The video camera was mounted to pick up the figure 12 on side of the test section and for the figures 13-15 inside the test section with a view orthogonal to the sheet of light. Figure 12 shows in comparison with the measured data pictured in figure 9 the four turns of the spiral shear layer. The following series of pictures shows the spiral form of this

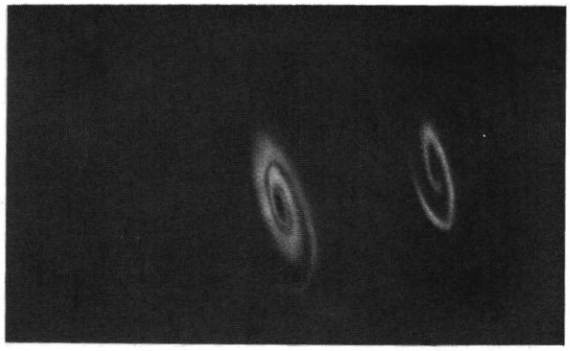

Fig. 12: Side view of the vortex at a delta-wing model. Test parameters: U_∞ = 20m/s, α = 28° x/ℓ = 0.614. (vortex breakdown point: x/ℓ = 0.73)

vortex from far upstream until near to the point of vortex breakdown. The dark parts in the vapor screen shows the vortex core, there the radial acceleration produced by circulatory flow exerts a strong centrifuging action on the smoke particles. As a consequence, these particles are usally quickly swept from the center of the vortex and creating a dark region. Also by small sizes of particles dark regions between the shear layer are visible. This effect especially is visible for a well defined ratio of particle sizes to centrifugal forces from this vortex. Another detail of the structure inside a vortex is shown in figure 13.

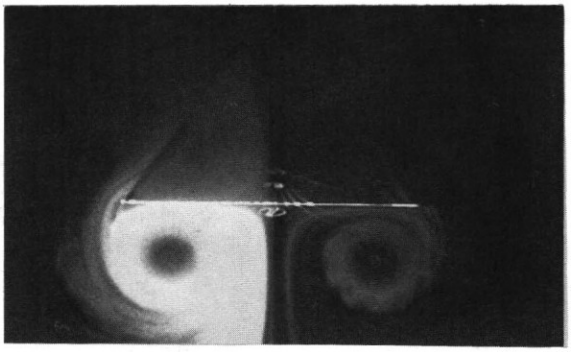

Fig. 13: Orthogonal view of the vortex at a delta-wing model.
Test parameters: Ma = 0.4, α = 20°, x/ℓ = 0.69 (vortex breakdown point: behind the wing)

By using coexistent different particle sizes the photographs give very different informations. In contrast to figure 12 the small particles in the vortex core create a small region of a dark core bordering on a white region. Some of the larger particles and the small ones build the outer white region, well to be seen on the right side vortex. Furthermore a structure on the shear layer is visible. After changing the ratio of small and large particles the wavy structure on the shear layer is marked. At the left side vortex there is a mixture of smaller and larger particle sizes and the right side gives an impression by using only large particles.

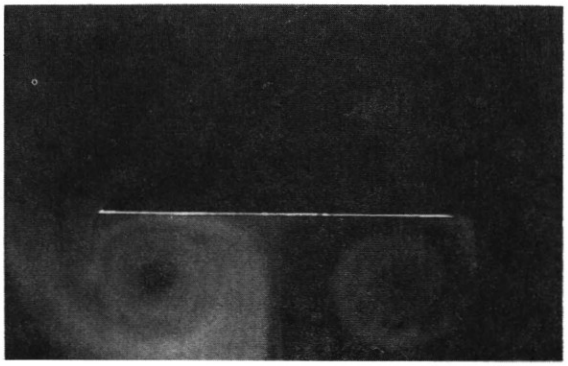

Fig. 14: View and test parameters as figure 13 but changing the particle sizes and conditions

Observations showed that the vortex sheet were not caused by the vibration of the delta wing. The video film gives detailed information about the "pseudo-stationary" instabilities. The assumption is, that some of the small reproducible kinks in the curve - see figure 8 - obtained by the opto-acoustical method will be created by this instabilities. The shift of the light sheet shows a constant structure on the surface of the shear layer. It is possible to determine the slope angle of surface instabilities in dependence on the distance x/ℓ. Furthermore the number of single-instabilities can be counted and the thickness of shear layer is predictable by the Helmholtz-instabilities. Figure 15 shows a digitized filtered video picture for clearly detection of the periodical structure of instabilities.

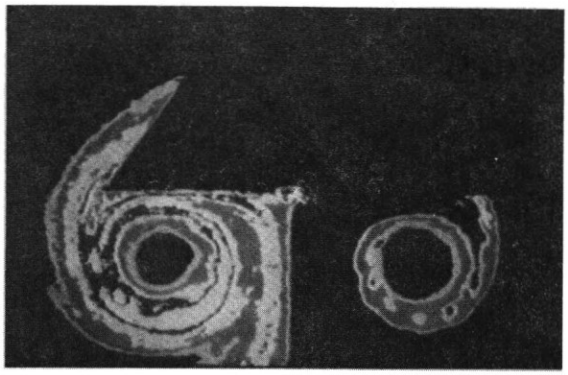

Fig. 15: Digitized filtered photograph for detection of instabilities. (Same Photograph as figure 14)

There the different grey scale produced by the smoke intensity was defined by the computer in variable colours.

Conclusion

The results of measurements in seven planes before the point of vortex breakdown gives detailed information on the velocity and circulation distribution inside a vortex. It has been shown that the region between the viscous core and the leading edge has four turns of the spiral shear layer. The jumps of circulation at each rotation were measured and there is potential flow between the turns of the spiral. Ludwieg's theory has been proven based on this information, which means that the shape parameter K falls below the critical value of 1.16 behind the point of vortex breakdown. Furthermore it can be shown, that instabilities on the shear layer are visible by using different sizes of smoke particles. The assumption is, that some of the reproducible kinks in the measured curve where created by this effect. The structure is "pseudo-stationary" for the instabilities on the shear layer in a constant plane over the wing. They will be produced at the vortex generation point and there propagation can be observed by a slope angle of the rolled up shear layer. By counting the wavelenghts of instabilities, the thickness of shear layer at different planes is predictable.

In summary we may draw the following conclusion for the opto-acoustic method:

- nondisturbing and quasi pointwise exploration of velocity (and temperature) is possible
- steady as well as unsteady flow fields can be determined
- very short measuring times can be attained
- no calibration is necessesary
- the structure of instabilities can be detected

Outlook

The final goal is to obtain an instantaneous picture of an entire plane inside a flow field. The concept of the measuring system is depicted in figure 16 . An array of ultrasonic transmitters (18 transducers, 3mm high) has been already developed. In addition, of course, an array of laser beams is required. Although completed in concept, which has been presented here, much work has still be done to implement the complete system with data aquisition, data reduction, numerical treatment and electronical equipment.
As shown in figure 16, this method can quasi "photograph" desired planes of the flow field. It provides an opportunity to investigate even unsteady flow fields. The complete instrumentation such as lasers, diodes and sound transmitters can be located outside of the test section of the wind tunnel, i.e. the flow field is undisturbed. Initial experiments have shown that the length of the integration path can be decreased to 5 mm. Comparing this approach with conventional pressure probes which interfere with the flow, we may state that the opto-acoustical method is superior.

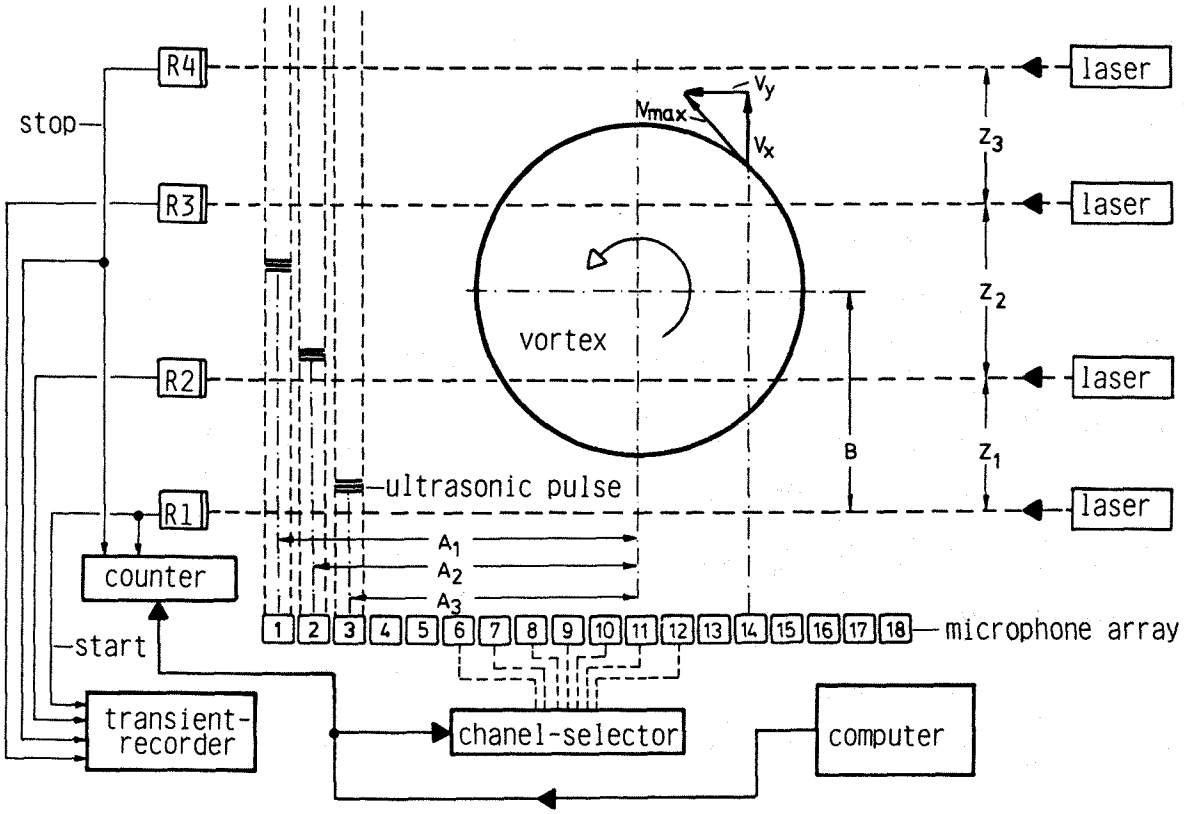

Fig. 16: Schematic diagram of the test setup for the first step to pick up an instantaneous picture of a whole plane inside a flow field

References

[1] Engler, R.H. Experimentelle Untersuchungen der Struktur und des "Aufplatzens" der Wirbel an einem angestellten schlanken Deltaflügel- ausgeführt mittels Ultraschall im Windkanal
Dissertation Göttingen (1986), Mathematisch-Naturwissenschaftliche Fachbereiche der Georg-August-Universität zu Göttingen

[2] Engler, R.H. Ultrasonic-Laser Method for Flow Field Measurements in Wind Tunnel Tests"
ICIASF'87 Record, (1987), 255-261

[3] Schmidt, D.W. "Acoustical Method for Fast Detection and Measurement of Vortices in Wind Tunnels"
ICIASF'75 Record, (1975), 216-228

[4] Ludwieg, H. Zur Erklärung der Instabilität der über Delta-Flügeln auftretenden freien Wirbelkerne Z. Flugwiss. 10 (1962), 242-249

[5] Hall, M. G. Vortex breakdown
Ann. Rev. Fluid Mech. 4 (1972), 195-218